

The Role of Electron-Donating Subunits in Cross-Linked BODIPY Polymer Films

Mücahit Özdemir, Baybars Köksoy, Bahattin Yalçın,* and Sermet Koyuncu*

A new method for synthesizing cross-linked

4,4-difluoro-4-bora-3a,4a-diaza-s-indacenes (BODIPYs) using a radical-based thiol-ene click reaction is developed. This method is simple, efficient, and cost-effective, and it produces polymers with unique optical, electrochemical, and surface morphology properties. Significant blue shifts in absorption and photoinduced electron transfer in emissions are observed in the cross-linked BODIPY thin films. Cross-linking also leads to the restriction of conjugation, which results in the breakage of the terminal vinyl group, an increase in the oxidation potential, and a slight upshift in the HOMO position. As a result, the electrochemical band gap is widened from 1.88 to 1.94 eV for polymer bearing *N,N*-dimethylamino-BODIPY and from 1.97 to 2.02 eV for polymer bearing *N,N*-diphenylamino-BODIPY moieties. Monomer thin films form planar surfaces due to crystallinity, while amorphous cross-linked BODIPY polymers form more rough surfaces. Additionally, photopatterning on the film surface is successfully performed using different patterned masks. This new method for synthesizing cross-linked BODIPYs has the potential to be used in a variety of applications, including organic electronics, bioimaging, and photocatalysis.

composite materials, and optical and electronic devices.^[1] In cross-linked polymers, targeted properties such as softness, hardness, electrical conductivity, biocompatibility, light resistance, and thermal stability vary depending on the type of cross-linker and the monomer used. Recently, the thiol-ene click reaction, which is a simple, inexpensive, and fast technique, has become an ideal covalent cross-linking polymerization technique.^[2] Side reaction problems encountered in classical polymerization were largely overcome by UV-light-mediated thiol-ene click reaction. The simplicity of the thiol-ene click reaction has opened up a new field for researchers in surface polymerization and has made a significant contribution to the rapid development of thin-film technologies.^[3] Photopatterning is a technique that is used to create patterns on the film surface in the presence of activating light, and the type of materials used in photopatterning processes should

1. Introduction

Cross-linked polymers are a versatile class of materials with a wide range of applications. They are widely used in elastomers,

be application-dependent. Patterned films can be obtained by a very simple method as a result of crosslinking under light.^[4] Cross-linked polymers, carbon dots, organic azo dyes, and inorganic metal complexes are materials that can be used in photopatterning processes.^[5]

4,4-difluoro-4-bora-3a,4a-diaza-s-indacene (BODIPY) dyes are very attractive materials due to their excellent Stokes shifts, narrow absorption bands, sharp emissions, high fluorescence quantum yields, and excellent chemical and photo-stabilities.^[6] These properties of BODIPYs allow them to show high-intensity light emission and to be used as electron transfer agents in optoelectronic applications.^[7] BODIPY dyes are actively involved in many applications as biochemical labeling agents and light harvesters such as organic light-emitting diode (OLED)-photovoltaics. BODIPY has a wide range of substituents and derivatives due to the derivatization of aldehyde and pyrrole. In addition to molecules with conjugated structures containing BODIPY, conjugated polymers with BODIPY skeleton structures in the repeated unit are also present in the literature.^[8] One of the main ways to develop low bandgap conjugated molecules and polymers is the donor-acceptor (DA) approach. This approach is extremely important in controlling the electronic structure of conjugated molecules for electronic device applications, especially electrochromics and photovoltaics.^[9] BODIPY compounds absorb and emit at wavelengths shorter than 600 nm when they are not modified. If the absorption band can be raised above 600 nm,

M. Özdemir, B. Yalçın
 Department of Chemistry
 Marmara University
 Istanbul 34722, Türkiye
 E-mail: byalcin@marmara.edu.tr

B. Köksoy
 Department of Chemistry
 Bursa Technical University
 Bursa 16310, Türkiye

S. Koyuncu
 Department of Chemical Engineering
 Çanakkale Onsekiz Mart University
 Çanakkale 17400, Türkiye
 E-mail: skoyuncu@comu.edu.tr

 The ORCID identification number(s) for the author(s) of this article can be found under <https://doi.org/10.1002/marc.202300552>

© 2023 The Authors. Macromolecular Rapid Communications published by Wiley-VCH GmbH. This is an open access article under the terms of the Creative Commons Attribution License, which permits use, distribution and reproduction in any medium, provided the original work is properly cited.

DOI: 10.1002/marc.202300552

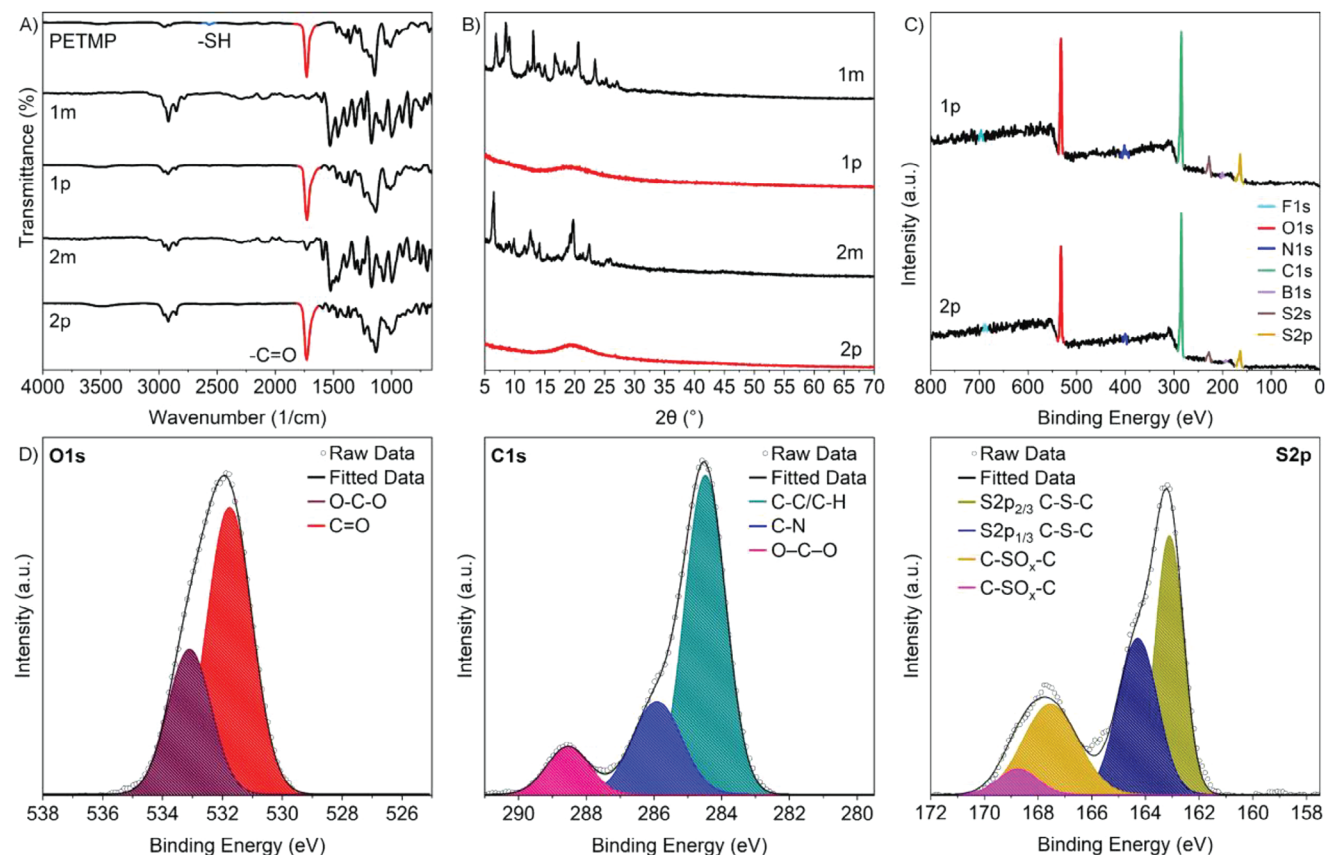


Figure 1. A) The FT-IR spectra of pentaerythritol tetrakis(3-mercaptopropionate), monomers (1m, 2m), and their crosslinked polymer (1p, 2p). B) The powder X-ray diffraction (XRD) curves of the crystallized (1m, 2m) and amorphous (1p, 2p) samples. C) The XPS survey and partial spectra of cross-linked BODIPY polymers (1p, 2p). D) The XPS high-resolution S2p, O1s, C1s, and S2p spectra of diphenylamino-BODIPY cross-linked polymer (2p).

this allows the use of these compounds in near-infrared (NIR) applications.

There are few studies on cross-linked polymers of BODIPYs. Xiao et al. synthesized fluorescent polymer probes with thermal stability via thiol-ene click reaction. It was determined that the polymers synthesized using thiol-based linkers also have very high fluorescence quantum yields. BODIPY polymers with high fluorescence intensity and fluorescence quantum yield were defined as good identifying probes for iron metal (Fe^{3+}). In addition, they stated that rigid-chain polymers exhibit higher fluorescence quantum yield and better thermal stability than flexible ones and that polymeric structures are more advantageous than monomers in spectrophotometric studies.^[10]

In this study, a radical-based thiol-ene click reaction, which is a simple, efficient, and cost-effective method for the synthesis of cross-linked BODIPY thin films, was used. Two different polymers containing donor units were synthesized and their structural properties were compared with the model compound that was previously published.^[11] Based on the results of this study, cross-linked BODIPY-containing thin films can be used in applications such as NIR electrochromic devices, microelectronics, sensors, LEDs, and solar panels. This work will be further developed and will be a steppingstone for scientists who are conducting research in this area.

2. Results and Discussion

New distyrene-BODIPY monomers (1m and 2m) were synthesized from their 2,6-dibrominated BODIPY derivatives (1b and 2b) and styrene boronic acid using the Suzuki–Miyaura cross-coupling reaction (Scheme S1, Supporting Information). The synthetic procedures, the structural characterization of monomers was completed by FT-IR, UV–vis, NMR (^1H , ^{13}C , ^{11}B , ^{19}F), and MALDI-TOF mass spectrometry, and all characterization details are given in the Supporting Information.

2.1. Structural Characterizations of Cross-Linked Polymers

Cross-linked polymers were characterized as FT-IR, SEM-EDX, TEM, powder X-ray diffraction (XRD), AFM, X-ray photoelectron spectroscopy (XPS), and TGA, spectrophotometrically and fluorometrically. Characteristic peaks of $\text{C}=\text{N}$, $\text{B}-\text{N}$, $\text{B}-\text{F}$, and $\text{C}-\text{N}$ vibrations were observed in the spectra of styrene-BODIPY compounds (1m, 2m). After the polymerization of the styrene bearing BODIPY and PETMP by thiol-ene click reaction, the small thiol ($-\text{SH}$) peak around 2560 cm^{-1} disappeared, and the carbonyl ($\text{C}=\text{O}$) peak at 1700 cm^{-1} belonging to the PETMP was observed in the 1p and 2p polymer spectra, as well as the peaks belonging to BODIPY compounds (Figure 1A).

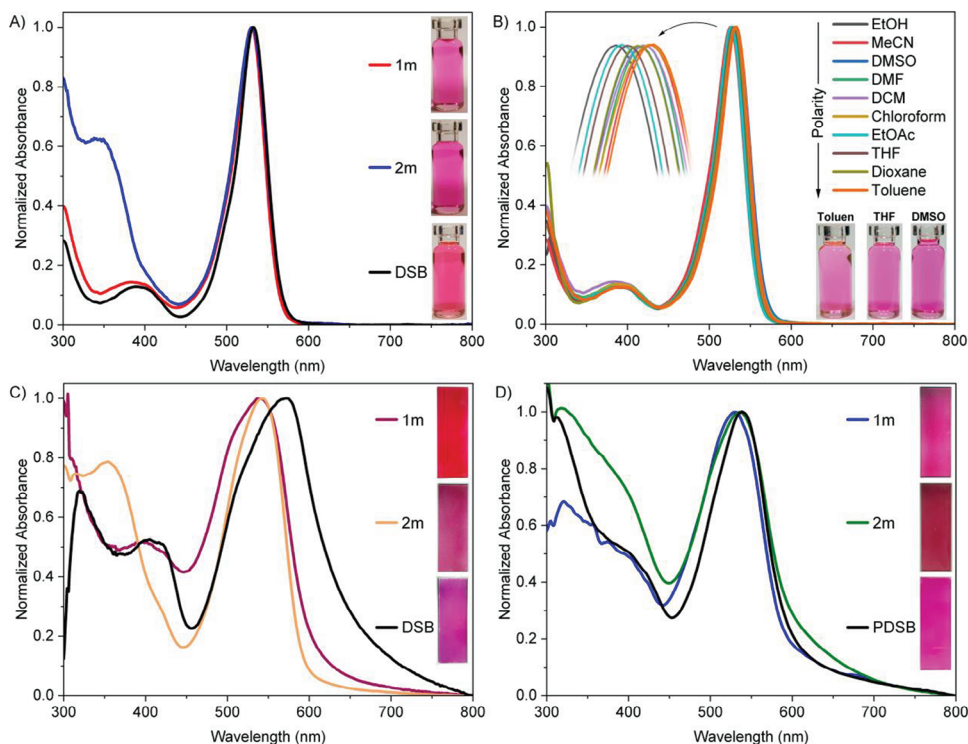


Figure 2. A) The comparative UV-vis spectra of BODIPY's (1m, 2m, and DSB) in dichloromethane. B) The UV-vis spectra of 1m in ten different solvents. C) The thin film UV-vis spectra of BODIPY monomers (1m, 2m, and DSB). D) The thin film UV-vis spectra of cross-linked BODIPY polymers (1p, 2p, and PDSB).

Powder XRD was used to analyze the structures of styrene-BODIPY compounds (1m, 2m) and crosslinked BODIPY polymers (1p, 2p). The XRD patterns of crystal BODIPYs showed distinct and severe diffraction peaks in the 5–30° (2θ) range, indicating that the samples are single crystals. However, because of the flexible nature of the crosslinker, the crystalline materials turned into an amorphous structure upon polymerization. This is because all monomers participate in the polymerization process, and no microcrystalline monomer remains in the polymer structure. As a result, no diffraction peaks belonging to crystalline structures appear in the polymeric spectra (Figure 1B).

C–S and C=O bonds are bonds found in cross-linked polymers 1p and 2p but not in monomers 1m and 2m. These bonds were investigated using the XPS method. When the XPS spectra of monomers and polymers are examined in a row, it is proven that polymerization has taken place with the presence of O 1s and S 2p signals after the thiol-ene click reaction (Figure 1C). In XPS spectra of dimethylamino and diphenylamino substituted BODIPY polymers (1p and 2p), signals were determined with binding energies of 191.8 for B 1s, 284.5 for C 1s, 685.2 for F 1s, 401.2 for N 1s, 531.8 for O 1s, and 227.9 and 163.9 eV for S 2s and S 2p. Detailed analysis of the partial spectrum for polymers indicates 531.8 eV C=O and 533.4 eV O–C–O bonds for O 1s. For C 1s, 284.3 eV indicates C–C/C–H, 285.1 eV C–N, and 288.7 eV O–C–O bonds. For S 2p, the range of 163.3 eV S 2p_{2/3} C–S–C, 164.5 eV S 2p_{1/3} C–S–C, 166–170 eV indicates oxidized sulfur bonds (Figure 1D). The partial spectra for B 1s, F 1s, and N 1s are provided in the Supporting Information. All these XPS anal-

yses showed that the polymerization took place in the expected direction.

2.2. Optical Properties

The UV-vis spectra of BODIPY compounds containing *N,N*-dimethylamino, and *N,N*-diphenylamino donor subgroups from the meso position in dichloromethane and solid state (thin film) were investigated. In the UV-vis spectra in DCM, the peak was measured as 530 nm for 1m, 531 nm for 2m, and 533 nm for 2,6-bis(4-vinylphenyl)–8-phenyl-1,3,5,7-tetramethyl-4,4-difluoro-4-bora-3a,4a-diaza-s-indacene (DSB). The monomers in the thin film absorption spectra are 540 nm for 1m, 530 nm for 2m, and 572 nm for DSB. The peak in thin film spectra of crosslinked polymers was measured as 530 nm for 1p, 540 nm for 2p, and 538 nm for DSB (Figure 2C,D). Solid-state spectra have a wider absorption band due to photons hitting multiple irregularly arranged molecules. To examine the absorption behavior of BODIPY compounds with good solubility in solvents with different polarities, absorption spectra were measured in ten different solvents at the same concentration. The band shapes did not change in the absorption spectrum of 1m and 2m in different solvents, but they shifted to blue in polar solvents and shifted to red in nonpolar solvents (Figure 2B).

The fluorescence spectra of BODIPY monomers (1m, 2m) and polymers (1p, 2p) in dichloromethane and solid state were investigated. All measurement concentrations were 1×10^{-6} M and all

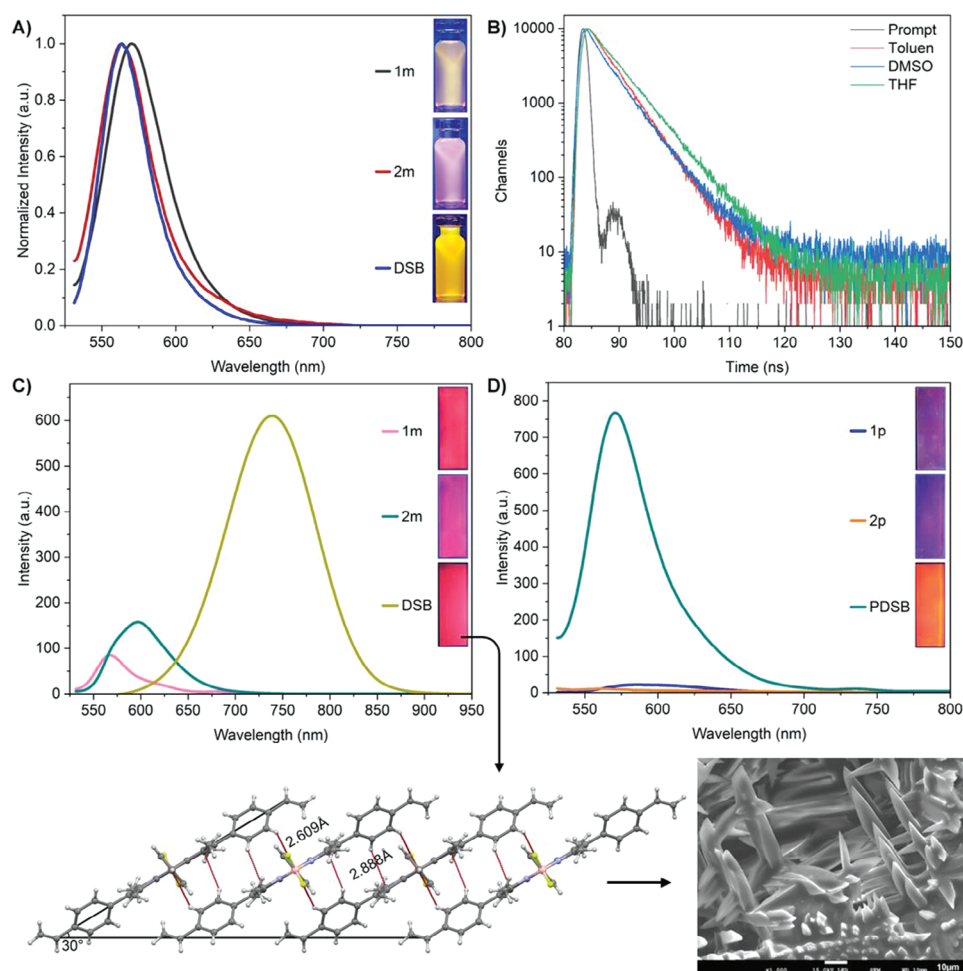


Figure 3. A) The comparative fluorescence spectra of BODIPYs (1m, 2m, and DSB) in dichloromethane. B) The lifetime spectra of 2m in Toluene, THF, and DMSO. C) The thin film fluorescence spectra of BODIPY monomers (1m, 2m, and DSB). D) The thin film fluorescence spectra of cross-linked BODIPY polymers (1p, 2p, and PDSB).

excitation wavelengths $\lambda_{\text{start}}^{\text{em}} = 520 \text{ nm}$ for BODIPY's. In DCM, 1m, 2m, and DSB exhibited similar emission spectra, but emission quenching was observed in 1m and 2m spectra due to photoinduced electron transfer (PET). Under normal conditions, the PET effect is expected to be in the BODIPY compound containing the $-\text{NMe}_2$ subgroup, which is the stronger donor group but surprisingly, the opposite situation occurred in DCM. While the $-\text{NPhe}_2$ group did not cause any shift in the emission peak, the 1m containing $-\text{NMe}_2$ subgroup was shifted to the 6 nm red region compared to the others. While high emission intensity was observed in the DSB compound in DCM, the emission of 1m was quenched, while the emission of 2m was quenched even more than 1m. The peaks of the emissions received in the solvent were measured as 570 nm for 1m, 564 for 2m, and 564 nm for DSB (Figure 3A).

The solvent effect has disappeared in the emission spectra of the thin films prepared by the spray method. Contrary to the solvent environment, 2m has a higher intensity and blue-shifted emission band in thin films, while the emission of 1m is quenched. In the compound DSB, π -stacks were formed due to micro-crystals and DSB's domino-like arrangement with

each other, and thus mega emission shift was observed. Cherumukil et al. and Tian et al. have similarly reported red-shifted or newly formed emission bands in photochromic π -extended BODIPYs.^[12] Due to the low crystallinity in the 1m and 2m thin films, mega stokes shift like in the DSB was not observed. The emission peaks of thin films of BODIPY monomers are 567 nm for 1m, 597 nm for 2m, and 757 nm for DSB (Figure 3C). The emission peaks of thin films of cross-linked BODIPY polymers are 586 nm for 1p (intensity 22.56 a.u.), 560 nm for 2p (intensity 11.33 a.u.), and 571 nm for PDSB (Figure 3D).

By using 1m and 2m monomers, the emissions of the polymeric surfaces formed as a result of the thiol-ene click reaction with the PEMTP cross-linker were almost completely quenched, unlike the monomers. The emission of the PDSB thin film is quite intense and unlike the monomer DSB, mega stokes shift was lost. As a result of cross-linking, the alkene double bond was opened, conjugation narrowing, reaction with the thiol group, and chain elongation resulted in increased emission. The reason why PDSB emits light but 1p and 2p compounds do not is that the donor $-\text{NMe}_2$ and $-\text{NPhe}_2$ subgroups in 1p and 2p compounds absorb the energy of BODIPY, preventing it from emitting light.

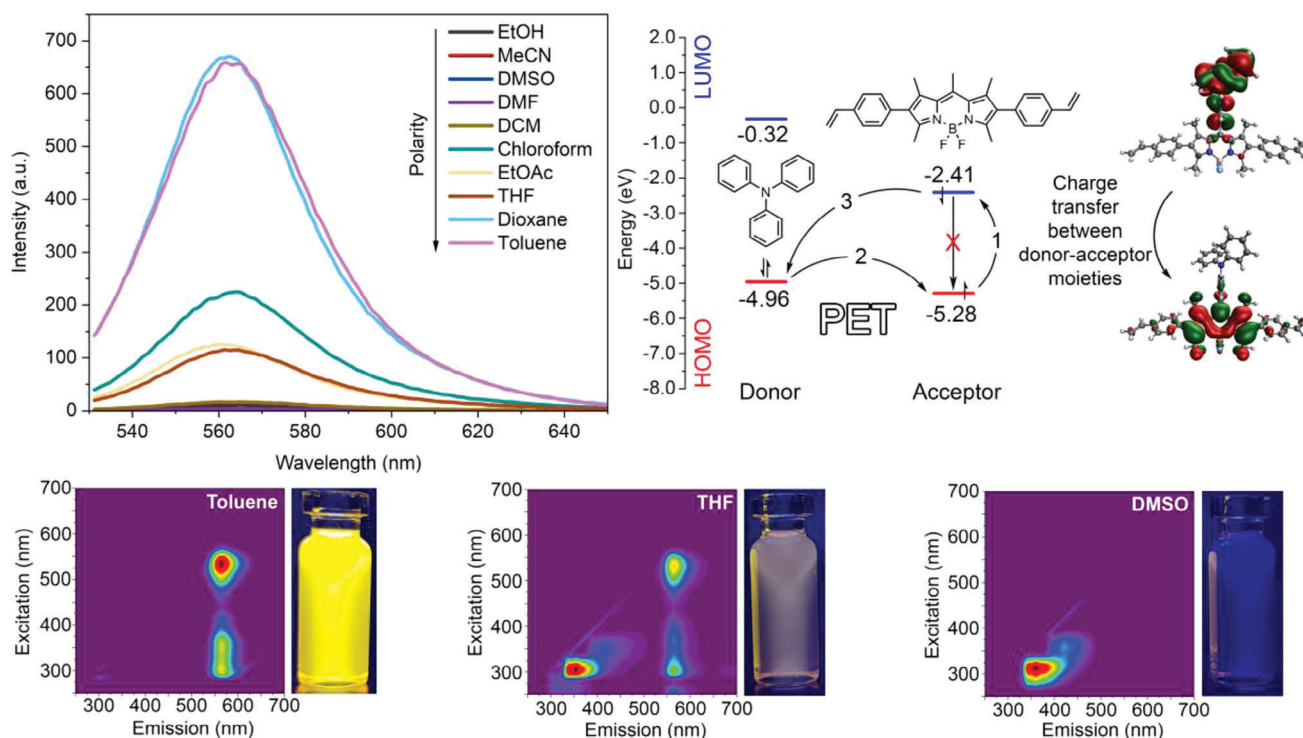


Figure 4. The emission spectra of 2m in ten different solvents and photoinduced energy transfer mechanism.

As the number of donor groups in the polymeric structure increased, the emission intensity decreased further.

The PET process of the monomers (1m, 2m) was demonstrated using the 3D fluorescence technique. In the PET mechanism, the HOMO energy levels of the $-NMe_2$ and $-NPh_2$ donor groups are higher than the HOMO energy level of the acceptor BODIPY dye. This means that electrons can easily pass from the LUMO orbital of BODIPY to the HOMO orbitals of the donor groups. Nonpolar toluene widens the band gap of the BODIPY compound, making it more difficult for electrons to pass from HOMO to LUMO. As toluene does not interact with BODIPY, PET was not observed. On the other hand, THF and DMSO narrow the band gap of BODIPY. As well as being aprotic, they interact with BODIPY, which facilitates the movement of electrons, facilitating the transition of electrons from HOMO to LUMO. This is why PET was seen in these solvents (**Figure 4**).

The fluorescence lifetime (τ_F) of styryl-BODIPY derivatives (1m, 2m) was measured in toluene, DMSO, and THF. Contrary to the fluorescence quantum yield, nonpolar solvents shortened the fluorescence lifetime, while polar solvents extended it. The lifetime values for 1m were 3.93 ± 0.015 ns in toluene, 4.01 ± 0.005 ns in THF, and 4.21 ± 0.008 ns in DMSO. The lifetime values for 2m were 3.89 ± 0.005 ns in toluene, 4.36 ± 0.012 ns in THF, and 4.69 ± 0.006 ns in DMSO. Fluorescence quantum yields (Φ_F) of styrene-BODIPY compounds (1m, 2m) were measured in toluene, DMSO, and THF. Fluorescence quantum yields of 1m were determined as 0.57 for toluene, 0.03 for THF, and 0.02 for DMSO, while fluorescence quantum yields of 2m were determined as 0.65 for toluene, 0.10 for THF, and 0.03 for DMSO. The fluorescence quantum yields of BODIPY compounds contain-

Table 1. The photophysical parameters of BODIPY compounds (1m, 2m) and the cross-linked BODIPY polymers (1p, 2p).

	Type	$\lambda_{\text{max}}^{\text{abs}}$	$\lambda_{\text{max}}^{\text{em}}$	$\Delta\nu^-$	Φ_F	τ_F
1m	Toluene	533	561	936	0.57	3.93
	THF	530	564	1137	0.03	4.01
	DMSO	532	563	1035	0.02	4.21
	Solid	544	567	746	–	–
2m	Toluene	533	563	1000	0.65	3.89
	THF	530	563	1106	0.10	4.36
	DMSO	533	565	1063	0.03	4.69
1p	Solid	537	586	1557	–	–
	Solid	537	560	765	–	–

ing the $-NMe_2$ and NPh_2 subunit are high in nonpolar toluene due to the intense emission. However, the fluorescence quantum yields are considerably lower in medium polar THF and polar DMSO due to photo-induced energy transfer, also known as emission quenching. The fluorescence quantum yields (Φ_F) and lifetimes (τ_F) of BODIPY's in toluene, THF, and DMSO are positively correlated with each other. The photophysical parameters of all compounds are provided in **Table 1**.

2.3. Theoretical Studies

The optimized geometries of dimethylamino-styrene-BODIPY (1m) and diphenylamino-styrene-BODIPY (2m) compounds

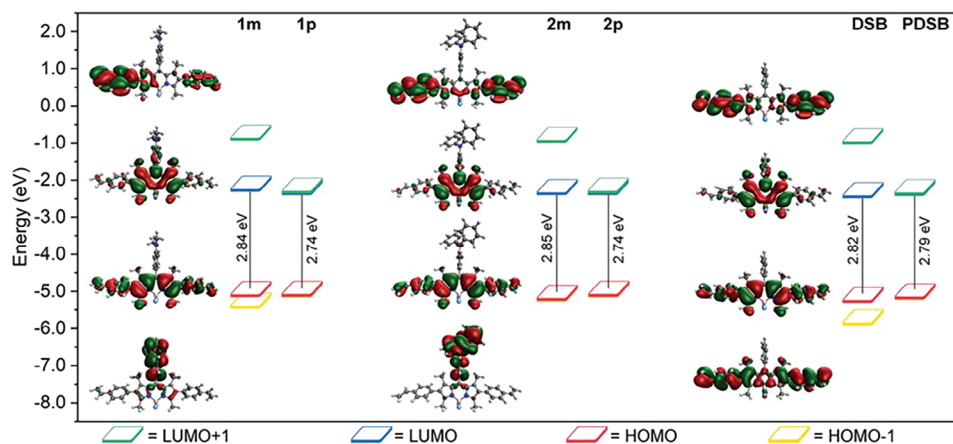


Figure 5. Calculated band gap values and molecular orbitals of styrene-BODIPY compounds (1m, 2m, and DSB) containing phenyl, *N,N*-dimethylamino, and *N,N*-diphenylamino subgroups and their cross-linked polymers (1p, 2p, and PDSB).

show that the phenyl ring connected from the meso position in 1m is positioned at an angle of 76.48° to the BODIPY skeleton, while in 2m, it is positioned at an angle of 90.80°. The styrene groups attached at the beta positions are positioned opposite to each other, with an average angle of 52.50° to the BODIPY skeleton. The average angle between the C–N–C atoms belonging to the dimethylamino and diphenylamino groups is 119°, and the C–N bond length is 1.454 Å. The angle between F–B–F atoms is 110.49°, and the B–F bond length is 1.394 Å. The angle between the N–B–F atoms is 110.50°, and the N–B bond length is 1.557 Å. The bond length of the terminal alkene groups is 1.35 Å. For cross-linked polymers (1p, 2p), the length of the C–C bond is 1.540 Å, while the length of the C–S bond is 1.839 Å after the alkene double bond is opened through the thiol-ene click reaction.

The calculated molecular orbitals of the dimethylamino-styrene-BODIPY compound (1m) show that the HOMO-1 orbital is located on the meso-position donor *N,N*-dimethylaminobenzene with a value of –5.44 eV. The HOMO orbital is directed toward the BODIPY-centered styrene groups (–5.13 eV). The LUMO orbital is situated at the BODIPY center (–2.29 eV), while the LUMO+1 orbital is found on the styrene groups (–0.91 eV). For the diphenylamino-styrene-BODIPY compound (2m), the HOMO-1 orbital is located on the meso-position donor *N,N*-diphenylaminobenzene subunit (–5.25 eV). The HOMO orbital is directed toward the BODIPY-centered styrene groups (–5.23 eV). The LUMO orbital is situated at the BODIPY center (–2.38 eV), while the LUMO+1 orbital is found on the styrene groups (–0.97 eV). For both BODIPYs, the orbitals from HOMO-1 to LUMO+1 show ordered charge transfer, indicating energy transfer (Figure 5).

The band gap values of the compounds were 2.82 eV for DSB, 2.84 eV for dimethylamino-styrene-BODIPY compound (1m), and 2.85 eV for diphenylamino-styrene-BODIPY compound (2m). The band gap widened slightly as the electron-donating increased, but it was still observed that the addition of donor subgroups from the meso position did not significantly affect the band gap. For the cross-linked polymers (1p, 2p) obtained from two dimethylamino- or diphenylamino subunit substituted BODIPY monomers, the HOMO-1, HOMO, LUMO, and

LUMO+1 orbitals were situated at the center of BODIPY. The calculated band gap of polymer 2p is 2.74 eV. The band gap of PDSB is 2.81 eV. The calculated band gaps of 1p and 2p are 2.84 and 2.85 eV, respectively. The polymers exhibit ambipolar behavior, and as the PETMP group does not contribute to the orbitals, they are potential candidates for use as conductive materials in optoelectronic applications.

2.4. Electrochemical Properties

Electrochemical characterization of styrene-BODIPY and their cross-linked polymers were carried out via cyclic voltammetry (CV) and differential pulse voltammetry (DPV) techniques in 0.1 m TBAPF₆/DCM electrolyte solution (Figure 6).

In the anodic scan, the pendant *N,N*-dimethylamino, and *N,N*-diphenylamino donor groups located next to the conjugated main chain are oxidized by giving electrons. The diphenylamino side group is a better electron donor, so the oxidation potential of the 2m structure is slightly reduced compared to the 1m structure. In the cathodic scan, the BODIPY group is reduced by accepting electron/s. The reduction potential is around $E_{1/2}^{\text{cathodic}} = -1.2$ V. This value shows that the BODIPY group is a good electron acceptor.

The cross-linking resulted in the breaking of the terminal vinyl group and the limitation of conjugation, which led to an increase in the oxidation potential and a slight upward shift in the HOMO position. As a result, the HOMO–LUMO band gap values were calculated as 1.88 and 1.97 eV for monomers and 1.94 and 2.02 eV for polymers. These data are in good agreement with the optical and theoretical band gaps. As a result, the modifications made by changing the donor groups in the structure have made it possible to easily adjust the HOMO and LUMO positions in the synthesized structures. The electrochemical parameters of all compounds are provided in Table 2.

2.5. Thermal and Photo-Resistance Analysis

The thermal behavior of *N,N*-dimethylamino-styrene-BODIPY (1m) and *N,N*-diphenylamino-styrene-BODIPY (2m) and their

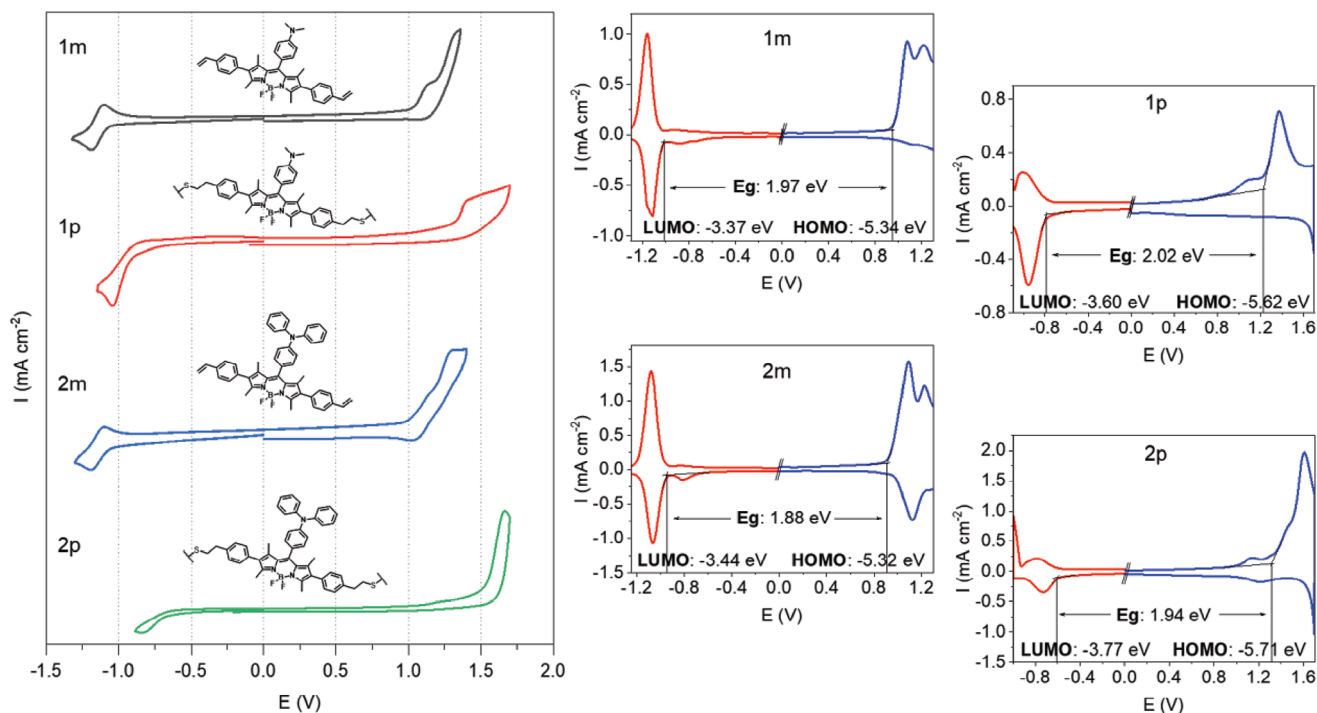


Figure 6. The cyclic voltammetry (CV) and differential pulse voltammetry (DPV) spectra of 1m and 1p in 0.1 M DCM/TBAPF₆ electrolyte solution at 100 mV s⁻¹ Ag wire scanning rate.

cross-linked polymers (1p and 2p) was investigated. 1m lost 5% mass between 13 and 29 °C, which was associated with breaking terminal alkene groups. Between 37 and 64 °C, 41% mass loss was observed due to the breaking of alkene-free benzene rings attached to carbons in beta positions of BODIPY. The strongest decay event occurred at 44 °C. Polymer 1p degraded from 19 to 65 °C and showed a mass loss of 74%. The strongest decay event occurred at 32 °C. 2m exhibited similar thermal behavior to 1m. There was a 4% mass loss from 12 to 27 °C and a 46% mass loss from 39 to 62 °C. The strongest decay event was observed at 43 °C. Polymer 2p decomposed from 19 to 60 °C and showed a mass loss of 66%. The strongest decay event occurred at 43 °C. At 80 °C, 52.83% and 47.78% residues of molecules 1m and 2m, respectively, show that these compounds have very stable structures

Table 2. The electrochemical parameters of BODIPY compounds (1m, 2m) and the cross-linked BODIPY polymers (1p, 2p).

	Reduction peak potential	Oxidation peak potential	E_{HOMO}	E_{LUMO}	$E_{\text{GAP}}^{\text{Elect}}$	$E_{\text{GAP}}^{\text{Optic}}$	$E_{\text{GAP}}^{\text{DFT}}$
1m	$E_{\text{m,c}}^{\text{red}} = -1.16$ $E_{\text{m,a}}^{\text{red}} = -1.11$	$E_{\text{m,c}}^{\text{ox1}} = 1.07$ $E_{\text{m,c}}^{\text{ox2}} = 1.22$	-5.34	-3.37	1.97	2.20	2.84
1p	$E_{\text{m,c}}^{\text{red}} = -1.01$ $E_{\text{m,a}}^{\text{red}} = -0.96$	$E_{\text{m,c}}^{\text{ox1}} = 1.11$ $E_{\text{m,c}}^{\text{ox2}} = 1.38$	-5.62	-3.60	2.02	2.10	2.74
2m	$E_{\text{m,c}}^{\text{red}} = -1.08$ $E_{\text{m,a}}^{\text{red}} = -1.07$	$E_{\text{m,c}}^{\text{ox1}} = 1.09$ $E_{\text{m,c}}^{\text{ox2}} = 1.23$ $E_{\text{m,a}}^{\text{ox}} = 1.13$	-5.32	-3.44	1.88	2.15	2.85
2p	$E_{\text{m,c}}^{\text{red}} = -0.78$ $E_{\text{m,a}}^{\text{red}} = -0.72$	$E_{\text{m,c}}^{\text{ox1}} = 1.14$ $E_{\text{m,c}}^{\text{ox2}} = 1.61$ $E_{\text{m,a}}^{\text{ox}} = 1.22$	-5.71	-3.77	1.94	2.05	2.74

compared to their polymers. The monomers generally exhibited similar thermal behavior, and it was observed that the addition of donor subgroups from the meso position did not significantly affect the thermal stability. The presence of 22.32% and 28.23% residues of polymers 1p and 2p, respectively, indicates that these polymers are more unstable compared to their monomers, originating from flexible and long-chain crosslinkers (Figure 7).

The resistance of distyrene-BODIPY monomers (1m, 2m) and polymers (1p, 2p) thin films to 365 nm UV light was investigated at room temperature for up to 80 min. The photodegradation behavior of monomers and polymers showed significant

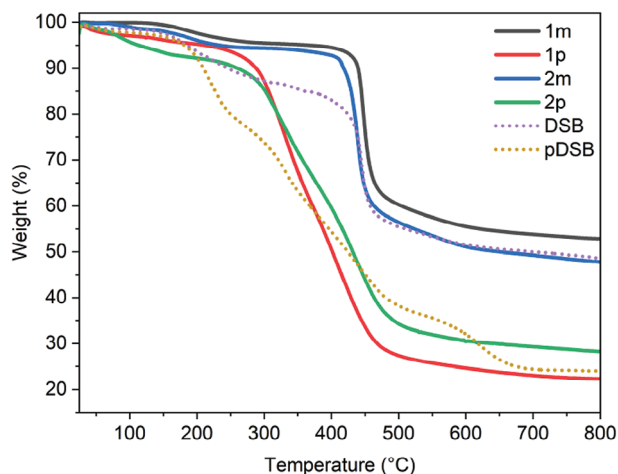


Figure 7. Thermogravimetric analysis (TGA) spectra of styrene-BODIPY monomers (1m and 2m) and their crosslinked polymers (1p and 2p).

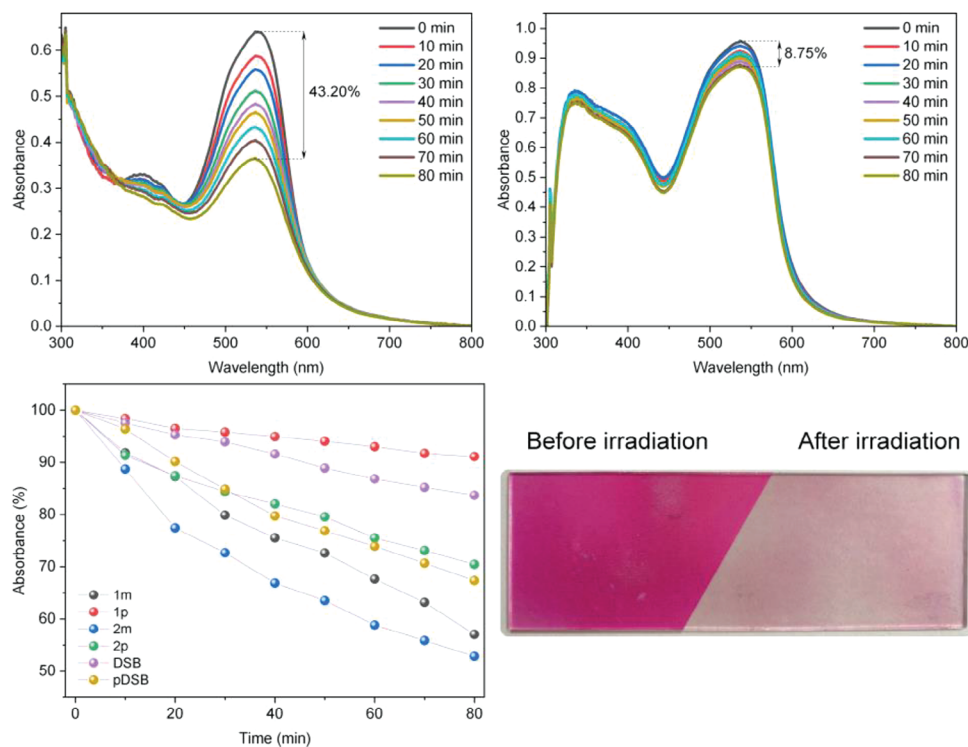


Figure 8. Photo resistance spectra of dimethylamino-distyrene-BODIPY (1m) and its cross-linked polymer (1p) against 100 W cm^{-2} UV light (365 nm) irradiation.

differences in their absorption spectra over time (Figure 8). The band at about 540 nm, which is the π - π^* transition for BODIPY, decreased sharply over time at the same light intensity, while the n - π^* band in the range of 300–400, decreased slightly due to its low energy. Monomers are less resistant to light than their polymers, contrary to thermal stability. In polymers, the cross-linked polymer containing the dimethylamino sub-group (1p) is more resistant to light than its derivative containing the diphenylamino sub-group (2p). BODIPY polymers formed with thiol-based linkers reduced the sensitivity of BODIPYs to light and delayed the degradation and decomposition of BODIPYs.

2.6. Thin Films and Photopatterning

Photopatterning studies of cross-linked polymers of styrene-BODIPY derivatives (1m, 2m) were carried out on a glass surface. The crosslinker PETMP and styrene-BODIPY mixture dissolved in chloroform were spin-coated onto the glass surface. A patterned mask was then placed on the glass film and exposed to 366 nm UV light. The thiol-ene click reaction took place in the areas exposed to UV light, and the pattern on the mask remained insoluble due to polymerization on the glass surface. The glass surface was then washed with chloroform to remove the non-polymerizable parts (Figure 9).

After the cross-linked polymerization of the fluorophore BODIPY monomers (1m, 2m) on the surface, their emissions were quenched due to photoinduced energy transfer. The patterns of the masks used in the photopatterning process were obtained down to the smallest detail on the glass surface.

2.7. Surface Morphology of Cross-Linked Films

Generally, crystalline molecules form smoother surfaces than amorphous molecules. The smooth surfaces of the styrene-BODIPY compounds (1m, 2m) are due to the planar and crystalline structure of the BODIPY core of the macrocyclic compound on the glass surface. Due to intermolecular interactions, crystalline BODIPY monomers are more uniformly and smoothly positioned on the glass surface. The vinyl group, a sub-unit of the styrene group, gives rise to non-covalent interactions between molecules, such as hydrogen bonding, van der Waals interactions, or dipole-dipole interactions. In addition, the tendency of the molecules to aggregate due to the active vinyl group has resulted in the formation of some defects, such as bumps or pits, on the film surface. Gap (pit) defects have also occurred during film formation by the spraying method, due to the removal of solvents and air.

When the AFM images of cross-linked BODIPY polymer (1p, 2p) films were examined, it was observed that agglomerations occurred on the film surfaces and rougher surfaces were formed. This roughness is because the BODIPYs are tightly held together by the crosslinker and randomly form interlocking cross-linked polymer chains. In addition, due to the random distribution of cross-links, the polymers on the film surface can be of different hardness and density, while polymerization proceeds in the form of porous or straight chains. The number of monomers contained in the segmented polymers on the surface also varies (Figure 10). The RMS roughness (R_q) values were determined as 3.50 nm for 1m, 11.57 nm for 1p, 3.88 nm for 2m, and 9.76 nm for 2p.

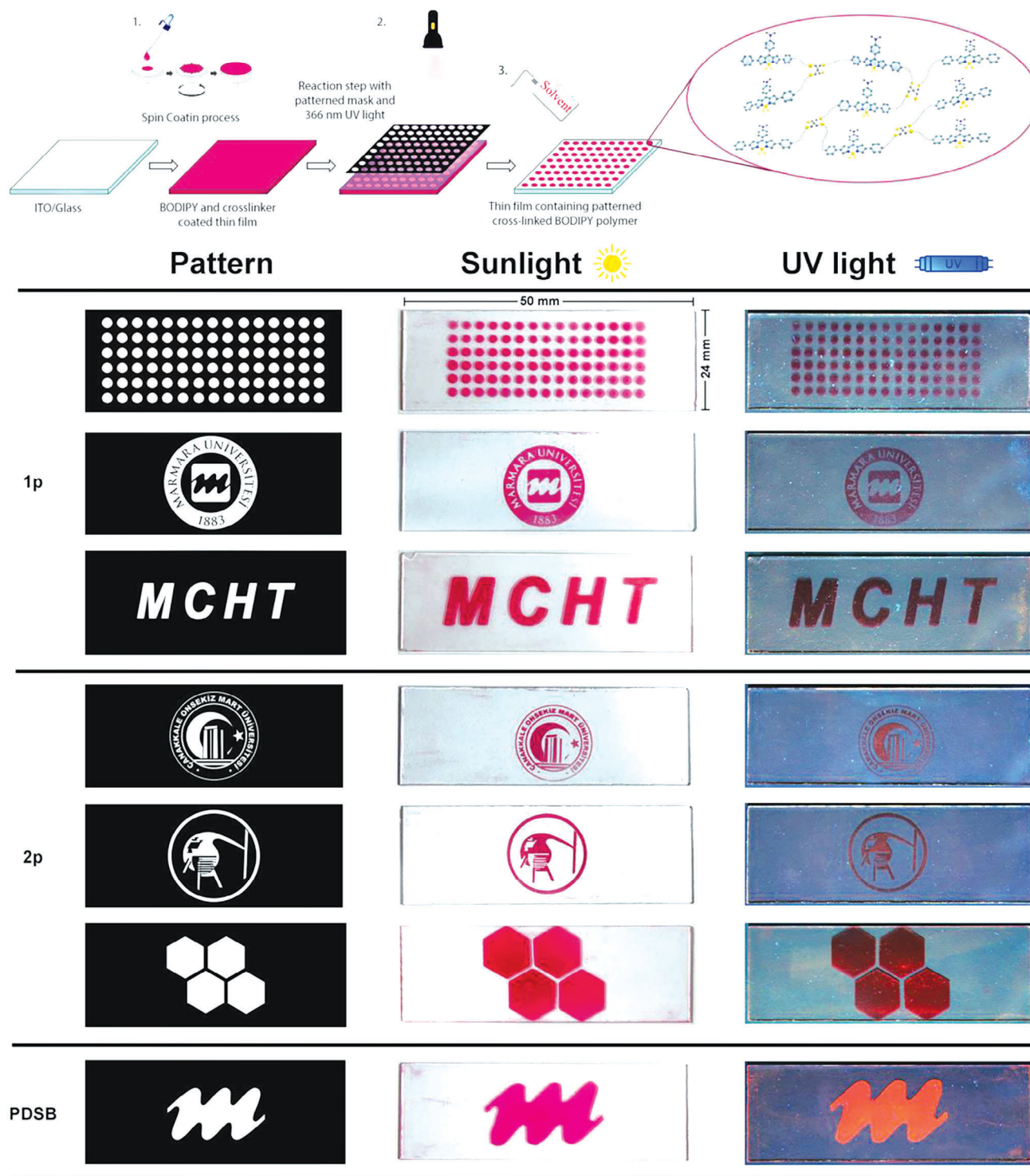


Figure 9. The photopatterning process and patterned BODIPY polymeric thin films under sunlight, UV light, and heatmap.

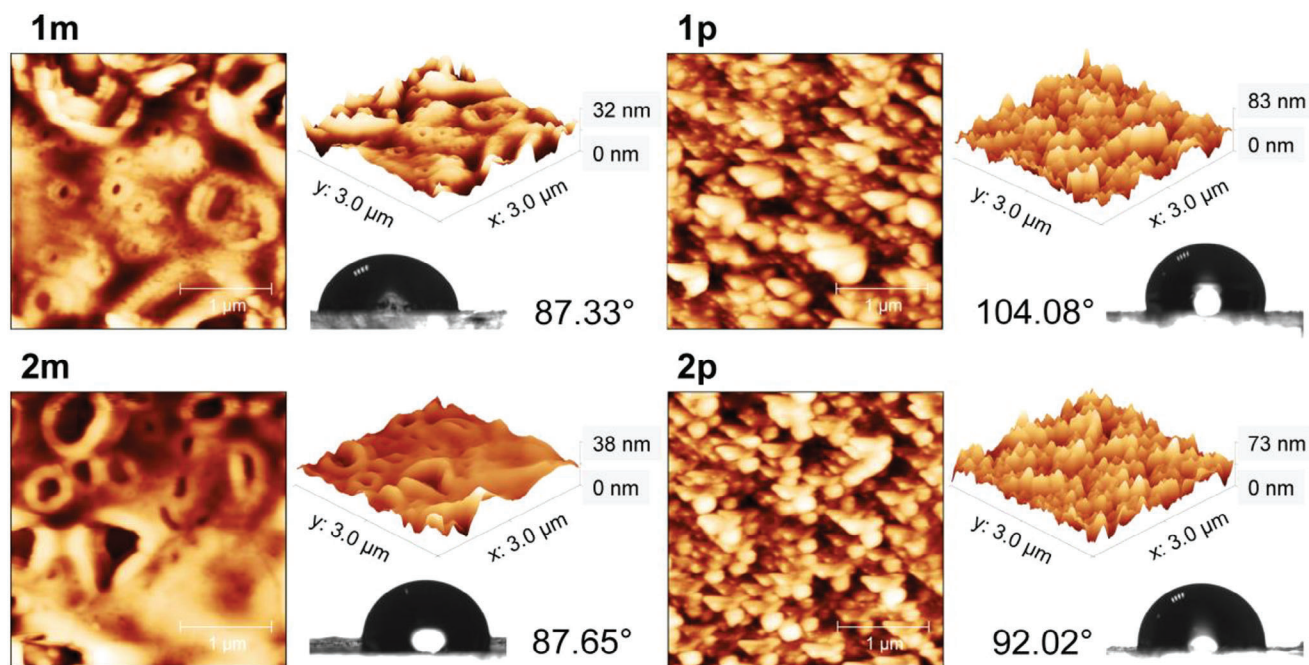


Figure 10. Atomic force microscopy (AFM), and contact angles of distyrene-BODIPY (1m and 2m) and their cross-linked polymers (1p and 2p) on thin film.

Styrene-BODIPY compounds (1m, 2m) are more hydrophilic than polymers (1p, 2p) due to the smooth surfaces of the monomers. As a result of polymerization, the hydrophobicity of the film surfaces of two polymers increased. A dramatic increase was observed in the dimethylamino-BODIPY polymer (1p), from 87.33° to 104.08° (Figure 10). Hydrophobic films are a desirable property in terms of water resistance. In polymer chemistry, long-chain or nonpolar materials are generally used to impart hydrophobic properties, but it is advantageous to obtain hydrophobic films without using any chain groups with BODIPY molecules.

SEM plots show that monomers have different crystal areas. As a result of crosslinking, the introduction of the flexible tetra thiol-based crosslinker into the structure reduced these crystal areas. In addition, the EDX analysis spectra for monomers showed the presence of carbon (C), nitrogen (N), boron (B), and fluorine (F) elements. In addition to these elements, polymers also showed the presence of oxygen (O) and sulfur (S) atoms, which are part of the crosslinker structure.

The dimethylamino-styrene-BODIPY (1m) and diphenylamino-styrene-BODIPY (2m) compounds, which are less prone to crystallization, formed smooth and regular surfaces. The compound 2m has a rougher surface than 1m due to stacking caused by the extra two benzene rings it contains. After the material is sprayed onto the surface, nanoscale voids and air bubbles are observed as a result of the evaporation of DCM. Amorphous surfaces were formed because of polymerization, and significant nanoscale polymerizations were observed in both 1p and 2p cross-linked polymers. When all SEM and TEM images are examined, it is clearly seen that the surface morphologies of the monomer and polymers change significantly after the thiol-ene click reaction and are correlated

with each other (Figure 11). SEM images are also supported by optical microscopy and AFM images.

All active layers of monomers exhibited homogeneous and thin nanostructures with different domain sizes. As a result of cross-linked polymerization, BODIPYs form discrete and bulky chains, which are seen in a spherical structure. In the TEM images of dimethylamino-styrene-BODIPY (1m) and diphenylamino-styrene-BODIPY (2m) compounds, monomers aggregate to form dark nebula images and inter-aggregate, or intra-agglomerate pores are observed in places. The significant difference between the monomer and polymer TEM morphologies, and the agreement with the SEM images, indicate that the polymerization has taken place without any problems. TEM images of all compounds are given in Figure 11.

3. Conclusion

In this study, we synthesized distyryl-BODIPY monomers containing donor sub-groups and used a radical-based thio-ene click reaction to create cross-linked BODIPY polymers on a thin film surface. This method is fast, efficient, and cost-effective, and the resulting materials have promising optical-electrochemical properties and surface morphology. The absorption spectra of the thin films shifted to blue due to the thiol groups, while their emissions were quenched by PET. The electrochemical band gap was widened from 1.88 to 1.94 eV for 1p and from 1.97 to 2.02 eV for 2p due to the broken conjugation. AFM and XRD images revealed that the flatness and crystallinity decreased due to the long-chain linker, resulting in rough amorphous film surfaces. Photopatterning studies were also carried out to apply targeted patterns on the film surface with high resolution. Patterned thin

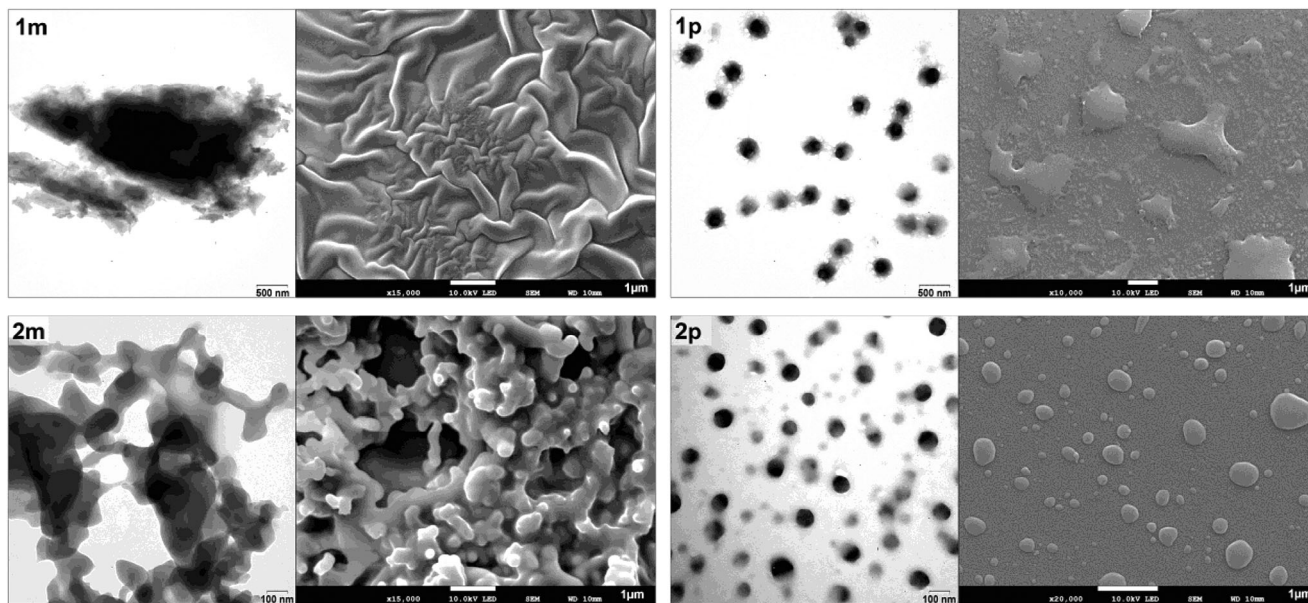


Figure 11. Scanning electron microscopy (SEM) and transmission electron microscopy (TEM) images of styrene-BODIPYs (1m and 2m) and their cross-linked polymer (1p and 2p) on thin film.

films can be used in applications such as NIR electrochromic devices, billboards, LEDs, and solar panels.

Supporting Information

Supporting Information is available from the Wiley Online Library or from the author.

Acknowledgements

This work was supported by the Research Foundation of Marmara University, Commission of Scientific Research Project (BAPKO) FDK-2022-10521. The numerical calculations reported in this work were fully performed at TUBITAK ULAKBIM, High Performance and Grid Computing Center (TRUBA resources).

Conflict of Interest

The authors declare no conflict of interest.

Data Availability Statement

The data that support the findings of this study are available in the supplementary material of this article.

Keywords

4,4-difluoro-4-bora-3a,4a-diaza-s-indacene, electron donating groups, optical properties, photopatterning, surface morphology, thiol-ene click

Received: September 15, 2023

Revised: October 18, 2023

Published online:

- [1] a) S. Rouif, *Nucl. Instrum. Methods Phys. Res., Sect. B* **2005**, 236, 68; b) J. P. Brutman, G. X. De Hoe, D. K. Schneiderman, T. N. Le, M. A. Hillmyer, *Ind. Eng. Chem. Res.* **2016**, 55, 11097; c) M.-H. Yoon, H. Yan, A. Facchetti, T. J. Marks, *J. Am. Chem. Soc.* **2005**, 127, 10388; d) Z. Wang, Q. Pan, *Adv. Funct. Mater.* **2017**, 27, 1700690; e) C. J. Kloxin, T. F. Scott, B. J. Adzima, C. N. Bowman, *Macromolecules* **2010**, 43, 2643.
- [2] C. E. Hoyle, C. N. Bowman, *Angew. Chem., Int. Ed.* **2010**, 49, 1540.
- [3] F. B. Koyuncu, A. R. Davis, K. R. Carter, *Chem. Mater.* **2012**, 24, 4410.
- [4] J. Jensen, A. L. Dyer, D. E. Shen, F. C. Krebs, J. R. Reynolds, *Adv. Funct. Mater.* **2013**, 23, 3728.
- [5] a) Y. Wang, X. Hao, H. Peng, X. Zhou, X. Xie, *Macromol. Rapid Commun.* **2022**, 43, 2100868; b) C. Wu, C. Li, X. Yu, L. Chen, C. Gao, X. Zhang, G. Zhang, D. Zhang, *Angew. Chem., Int. Ed.* **2021**, 60, 21521; c) H. Burgoon, C. Cyrus, D. Skilskyj, J. Thoresen, C. Ebner, G. A. Meyer, P. Filson, L. F. Rhodes, T. Backlund, A. Meneau, T. Cull, I. Afonina, *ACS Appl. Polym. Mater.* **2020**, 2, 1819; d) Y. J. Jeong, T. K. An, D.-J. Yun, L. H. Kim, S. Park, Y. Kim, S. Nam, K. H. Lee, S. H. Kim, J. Jang, C. E. Park, *ACS Appl. Mater. Interfaces* **2016**, 8, 5499; e) M. Zhang, J. Zhang, P. Alam, W. Li, J. W. Y. Lam, G. Jia, B. Z. Tang, *Adv. Funct. Mater.* **2023**, 33, 2213927.
- [6] A. Kamkaew, S. H. Lim, H. B. Lee, L. V. Kiew, L. Y. Chung, K. Burgess, *Chem. Soc. Rev.* **2013**, 42, 77.
- [7] M. Poddar, R. Misra, *Coord. Chem. Rev.* **2020**, 421, 213462.
- [8] A. Doshi, F. Jäkle, *Compr. Inorg. Chem. II* **2013**, 1, 861.
- [9] M. D. Yilmaz, T. Aytun, M. Frascioni, S. I. Stupp, J. F. Stoddart, *Synth. Met.* **2014**, 197, 52.
- [10] L. Xiao, C. Li, X. He, X. Cheng, *SN Appl. Sci.* **2021**, 3, 591.
- [11] M. Özdemir, S. Altınışık, İ. Ömeroğlu, B. Köksoy, M. Durmuş, B. Yalçın, S. Koyuncu, *ChemNanoMat* **2022**, 9, 202200295.
- [12] a) S. Cherumukkil, G. Das, R. P. N. Tripathi, G. V. PavanKumar, S. Varughese, A. Ajayaghosh, *Adv. Funct. Mater.* **2021**, 32, 2103041; b) D. Tian, F. Qi, H. Ma, X. Wang, Y. Pan, R. Chen, Z. Shen, Z. Liu, L. Huang, W. Huang, *Nat. Commun.* **2018**, 9, 2688.